

Preparation and Drug Loading of Poly(Ethylene Glycol)-*block*-Poly(ϵ -Caprolactone) Micelles Through the Evaporation of a Cosolvent Azeotrope

Karen K. Jette,¹ Devalina Law,² Eric A. Schmitt,² and Glen S. Kwon^{1,3}

Received January 22, 2004; accepted March 17, 2004

Purpose. The aim of this work was to study the assembly, drug loading, and stability of poly(ethylene glycol)-*block*-poly(ϵ -caprolactone) (PEG-*b*-PCL) micelles.

Methods. Three PEG-*b*-PCL compositions with PCL number average molecular weights of 1000, 2500, and 4000 g/mol were used. The assembly of PEG-*b*-PCL micelles, induced by the addition of water to acetonitrile (ACN), was characterized with ¹H nuclear magnetic resonance spectroscopy (¹H-NMR) and dynamic light scattering (DLS) with and without the presence of fenofibrate, a poorly water-soluble drug. PEG-*b*-PCL micelles with encapsulated fenofibrate were prepared through the removal of a negative ACN-water azeotrope under reduced pressure. Fenofibrate content was measured using reverse-phase high-performance liquid chromatography (HPLC), whereas the kinetic stability of PEG-*b*-PCL micelles with and without encapsulated fenofibrate was evaluated using size exclusion chromatography (SEC).

Results. The critical water content (CWC), the water content at which amphiphilic block copolymer (ABC) micelle assembly begins, was determined using DLS and ranged from 10% to 30% water, depending on both PCL molecular weight and PEG-*b*-PCL concentration. As the water content was increased, the PEG-*b*-PCL unimers assembled into swollen structures with hydrodynamic diameters ranging from 200 to 800 nm. The ¹H-NMR peaks associated with the PCL block exhibited line-broadening, following the addition of D₂O, indicating that the PCL blocks reside in the core of the PEG-*b*-PCL micelle. With further addition of water, the PCL cores collapsed to form fairly monodisperse PEG-*b*-PCL micelles (20–60 nm). In the presence of fenofibrate, the CWC value was lowered, perhaps due to hydrophobic interactions of fenofibrate and the PCL block. Further addition of water and subsequent evaporation of the negative ACN-water azeotrope resulted in fenofibrate-loaded PEG-*b*-PCL micelles of under 50 nm. The extent of fenofibrate encapsulation was dependent on PCL block size. At a polymer concentration of 1.0 mg/ml, PEG-*b*-PCL (5000:4000) and (5000:2500) micelles could encapsulate more than 90% of the initial loading level of fenofibrate, whereas PEG-*b*-PCL (5000:1000) micelles encapsulate only 28%. SEC experiments revealed that PEG-*b*-PCL (5000:4000) and (5000:2500) micelles eluted intact, indicating kinetic stability, whereas PEG-*b*-PCL (5000:1000) micelles eluted primarily as unimers.

Conclusions. PEG-*b*-PCL in ACN assembles with fenofibrate into drug-loaded polymeric micelles with the addition of water and the subsequent removal of a negative ACN-water azeotrope.

KEY WORDS: drug delivery; fenofibrate; poly(ϵ -caprolactone); poly(ethylene glycol); polymeric micelle.

¹ Division of Pharmaceutical Sciences, School of Pharmacy, University of Wisconsin-Madison, Madison, Wisconsin 53705, USA.

² Global Pharmaceutical Research and Development Division, Abbott Laboratories, Abbott Park, Illinois 60064, USA.

³ To whom correspondences should be addressed. (e-mail: gsk@pharmacy.wisc.edu)

INTRODUCTION

Recently, there has been much interest in polymeric micelles as drug carriers of poorly water-soluble and toxic drugs. Amphiphilic block copolymers (ABCs) have potential as drug delivery vehicles due to their ability to assemble into nanoscopic core/shell structures in a selective solvent (1–6). If the solvent is water, the core of the polymeric micelle is composed of the hydrophobic block and can be used as a depot for hydrophobic drugs (2,7). Commonly, poly(ethylene glycol) (PEG) has been used as the hydrophilic block in pharmaceutical applications because it is nontoxic and is FDA approved for parenteral use in humans (8). PEG is highly hydrated and flexible as the corona portion of the ABC micelle, and the high surface density of the PEG shell minimizes protein adsorption (9). This decreased protein adsorption leads to a reduction in uptake by the reticuloendothelial system (RES), allowing for enhanced blood circulation times (10,11).

Today, there are three major categories of PEG-micelles available for drug delivery based on the core-forming blocks: the triblock poloxamers or Pluronics comprising a poly(propylene oxide) (PPO) core, PEG-*b*-poly(L-amino acid)s, and PEG-*b*-poly(ester)s (12). Poly(ester)s are an attractive choice as a core-forming block because they are considered biocompatible and biodegradable. PEG-based poly(ester)s include PEG-*b*-PCL, poly(ethylene glycol)-*block*-poly(D,L lactic acid) (PEG-*b*-PDLLA), and poly(ethylene glycol)-*block*-poly(lactic-co-glycolic acid) (PEG-*b*-PLGA), all of which have been used as ABC micelles for the drug delivery of poorly water-soluble drugs (13–15).

Currently, there are three main approaches used to prepare drug-loaded ABC micelles: direct dissolution, solvent evaporation, and dialysis. The simplest technique to prepare drug-loaded polymeric micelles is using direct dissolution (7). At ABC concentrations above the critical micelle concentration (CMC), the ABC and the drug self-assemble in water to form drug-loaded ABC micelles. This method has been used to prepare drug-loaded Pluronics micelles. To enhance drug loading, this technique can be combined with an increase in temperature or the initial preparation of the drug as an evaporated film prior to the addition of Pluronics (16). If the drug-loaded ABC micelle cannot be prepared using direct dissolution, the solvent evaporation method can be used (17,18). With solvent evaporation, the ABC and the drug are dissolved in a volatile organic solvent, which is removed through evaporation, and a film consisting of ABC and drug is obtained. This film is then reconstituted with water, resulting in drug-loaded polymeric micelles.

Some ABCs are unable to form polymeric micelles using direct dissolution in water or after reconstitution following solvent evaporation. This generally occurs when the core-forming blocks are long and hydrophobic (e.g., PCL). Due to their hydrophobicity, such core-forming blocks are attractive for drug delivery purposes because of their ability to solubilize large amounts of poorly water-soluble drugs. In these cases, the dialysis technique has been used to prepare drug-loaded ABC micelles (19,20). Briefly, a solution of the drug and the ABC in an organic solvent is placed in a dialysis bag, with the molecular weight cutoff smaller than the size of the ABC. This bag is immersed into an aqueous environment,

and the organic solvent is exchanged with water, inducing ABC micelle assembly. Hydrophobic drugs can partition into the hydrophobic core of the ABC micelle during this assembly process. Using dialysis, ABC micelles based on PEG-*b*-PCL (Fig. 1A) have been used to successfully load poorly water-soluble drugs, including neurotrophic agents (21,22), indomethacin (23–25), dihydrotestosterone (13), and paclitaxel (26). However, we found the dialysis process was ineffective at loading certain drugs, such as fenofibrate, into PEG-*b*-PCL micelles. Fenofibrate (Fig. 1B) is a poorly water-soluble (~0.1 µg/ml) antihyperlipidemic agent (27,28). The encapsulation of fenofibrate into PEG-*b*-PCL micelles using the dialysis technique resulted in a loss of 75% of the initial loading level of fenofibrate during the dialysis process, rendering this technique ineffective.

We have hypothesized that an alternative method to remove the organic solvent may result in a high drug content within the PEG-*b*-PCL micelle. Therefore, new assembly conditions were developed to prepare PEG-*b*-PCL micelles. However, the assembly of PEG-*b*-PCL micelles using this technique was not well understood and required characterization. The purpose of this work was to describe and study PEG-*b*-PCL assembly, fenofibrate loading, and monitor the stability of PEG-*b*-PCL micelles. Because the length of the core-forming block can influence ABC micelle characteristics and drug-loading capabilities, this study used three compositions of PEG-*b*-PCL with varied PCL block sizes. PEG-*b*-PCL micelle assembly and fenofibrate loading was achieved by dissolving both PEG-*b*-PCL and fenofibrate in a volatile solvent, acetonitrile (ACN), and adding water to this solution. The negative ACN-water azeotrope was removed through rotary evaporation. Dynamic light scattering (DLS) and ¹H-NMR was used to characterize the assembly of PEG-*b*-PCL micelles, as a function of PEG-*b*-PCL concentration and PCL block length. The assembly of PEG-*b*-PCL in the presence of fenofibrate was also monitored with DLS as a function of PCL block size and PEG-*b*-PCL concentration. PEG-*b*-PCL micelles, with and without fenofibrate, were prepared. The dimensions of these micelles and their fenofibrate loading efficiency were determined with DLS and reverse-phase high-performance liquid chromatography (HPLC), respectively. The kinetic stability of PEG-*b*-PCL micelles, with

and without fenofibrate, was examined with size exclusion chromatography (SEC).

MATERIALS AND METHODS

Materials

Three compositions of PEG-*b*-PCL were purchased from Polymer Source Inc. (Montreal, Quebec, Canada). The length of the PEG block was constant at 5000 g/mol, whereas the PCL block length varied (1000, 2500, and 4000 g/mol) with M_w/M_n reported as 1.10, 1.25, and 1.28, respectively. ACN was reagent grade and purchased from Fisher Scientific (Fairlawn, NJ, USA). Milli-Q filtered water (Millipore Synthesis, Molsheim, France) was used in all experiments. Pyrene (purity 98%), acetonitrile-*d*₃ (ACN-*d*₃), and deuterium oxide (D₂O) were purchased from Aldrich Chemicals (Milwaukee, WI, USA). Dextran standards for SEC experiments were purchased from JM Science (Grand Island, NY, USA). PEG 8000, PEG 3350, and fenofibrate (purity >99%) were purchased from Sigma Chemical Co. (St. Louis, MO, USA).

Steady-State Fluorescence Measurements

Steady-state fluorescence measurements were used to calculate the critical micelle concentration (CMC) of PEG-*b*-PCL based on prior art (29,30). Pyrene was dissolved in acetone and aliquoted to test tubes, and the acetone was allowed to evaporate. PEG-*b*-PCL micelles were added to the test tubes, and the final concentration of pyrene was 1.25 µM. The fluorescence of pyrene was measured with a Hitachi F-3010 fluorescence spectrophotometer (Japan) at 25°C. The emission and excitation bandwidths were set to 3 nm with and a scan speed of 30 nm/min. The excitation spectra were collected between 300 and 400 nm at an emission wavelength of 390 nm. The fluorescence intensities at 334 and 339 nm were recorded, and their ratio was used to calculate the CMC for PEG-*b*-PCL micelles in water.

DLS

DLS experiments were performed using a NICOMP 380ZLS, Submicron Particle Sizer (Particle Sizing Systems, Santa Barbara, CA, USA) using the software CW380 version 1.61A to obtain the hydrodynamic radius of PEG-*b*-PCL micelles. For each sample, three separate DLS measurements were taken at 25°C. Each DLS measurement was taken for 12 min at a 90° angle with a wavelength of 639 nm. The data was analyzed in terms of volume-weighted distributions and interpreted using a Gaussian analysis. Because ACN and water mixtures were used, the viscosity and refractive index of the sample's solvent mixture was measured and used in each analysis.

Samples were prepared by dissolving each PEG-*b*-PCL composition in ACN and adding water gradually to obtain final PEG-*b*-PCL concentrations of 0.5, 1.0, or 2.0 mg/ml. Measurements were taken for samples with 0–90% (v/v) water in ACN at 10% water increments. The PEG-*b*-PCL samples were filtered through a 0.45-µm syringe filter.

To determine the effect of fenofibrate on PEG-*b*-PCL micelle assembly, an additional DLS study was performed.

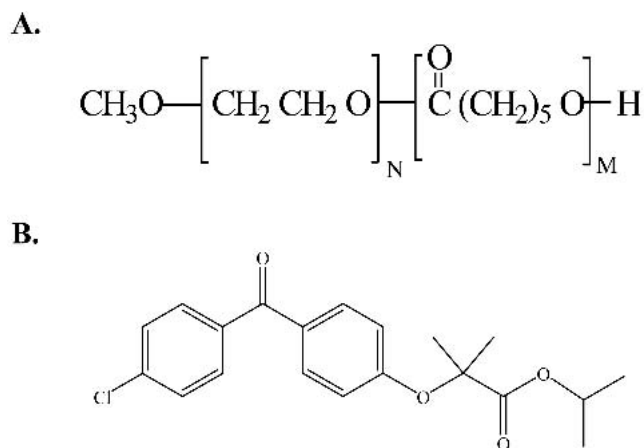


Fig. 1. (A.) Chemical structure of PEG-*b*-PCL. (B) Chemical structure of 2-[4-(4-chlorobenzoyl)phenoxy]-2-methylpropanoic acid 1-methylethyl ester (fenofibrate).

PEG-*b*-PCL and fenofibrate were dissolved in ACN and water was added to obtain final PEG-*b*-PCL concentrations of 0.5, 1.0, and 2.0 mg/ml. The final fenofibrate concentration was 10% of the initial weight of the PEG-*b*-PCL. The hydrodynamic diameters of PEG-*b*-PCL with the presence of fenofibrate were measured from 0–90% (v/v) water in ACN at 10% water increments.

¹H-NMR

A Varian INOVA 400Mz ¹H-NMR spectrometer equipped with VNMR software, version 6.0, was used for the acquiring and processing spectra (Varian, Palo Alto, CA, USA). Sample preparation was nearly identical to the procedure used for DLS measurements. Briefly, PEG-*b*-PCL (5000:4000) was dissolved in ACN-*d*₃. D₂O was added dropwise to obtain final D₂O-ACN-*d*₃ mixtures of 0–90% (v/v) D₂O in ACN-*d*₃ at 10% D₂O increments. The final PEG-*b*-PCL (5000:4000) concentration for each sample was 1.0 mg/ml.

ABC Micelle Preparation and Fenofibrate Loading

PEG-*b*-PCL was dissolved in ACN, and water was added gradually while stirring to reach at least 50% water content. The gradual addition of water to the dissolved ABC in organic solvent has been shown to result in small, spherical ABC micelles (31). Additional water was added to reach at least an 80% water content. Because water and ACN forms an azeotropic mixture at a composition 83.7% ACN with a boiling point of 76.5°C, this azeotropic mixture was easily evaporated leaving behind PEG-*b*-PCL micelles in water. The azeotrope was removed under vacuum at 37°C, and the resulting solution was subsequently filtered with a 0.22- μ m filter. Using reduced pressure, the azeotropic concentration was shifted to contain more ACN, thus allowing for rapid removal of the organic solvent (32), leaving PEG-*b*-PCL micelles in water.

To prepare fenofibrate loaded PEG-*b*-PCL micelles, both PEG-*b*-PCL and fenofibrate at 10% (w/w) were dissolved in 100% ACN. Water was added gradually until an 80% water content was achieved. Removal of the azeotrope and excess water was accomplished through rotary evaporation. The fenofibrate-loaded PEG-*b*-PCL micelles were filtered with a 0.22- μ m filter to remove excess fenofibrate that was not encapsulated. Final fenofibrate concentration before and after filtration was measured using HPLC.

HPLC

Measurements were performed using an Agilent 1100 series HPLC system equipped with Agilent ChemStation software (Agilent Technologies, Palo Alto, CA, USA). Samples were diluted with mobile phase consisting of ACN and water mixture (50:50 v/v), and 100 μ l of sample was injected onto an octadecyl silane column (“Little Champ” by Regis Technologies, Inc., Morton Grove, IL, USA) at 25°C. The fenofibrate content was determined using its absorbance at 288 nm. The samples were compared to standards containing known con-

centrations of fenofibrate (0.1–200 μ g/ml) dissolved in the mobile phase.

SEC

SEC measurements were performed using an Agilent 1100 series HPLC system equipped with a refractive index detector and analyzed with Agilent GPC software (Agilent Technologies, Palo Alto, CA, USA). PEG-*b*-PCL micelles, with and without encapsulated fenofibrate, were prepared using the assembly conditions described in “ABC Micelle Preparation and Fenofibrate Loading” above. Briefly, 100 μ l of the PEG-*b*-PCL micelle solution, with and without loaded fenofibrate, was injected onto a Shodex SB-806M HQ OHpak size exclusion column (Showa Denko, New York, NY, USA) at a concentration of 1.0 mg/ml. The flow rate was 0.8 ml/min, and the column temperature was 37°C. The results were compared with SEC chromatograms of dextran standards ($M_w = 1$ to 7×10^6 g/mol), PEG 8000, and PEG 3500 to achieve apparent molecular weights.

RESULTS AND DISCUSSION

PEG-*b*-PCL Assembly

The CMC values for PEG-*b*-PCL (5000:1000), (5000:2500), and (5000:4000) were determined experimentally using a pyrene probe (data not shown) and were 2.7, 0.74, and 0.2 μ mol/L, respectively. Therefore, PEG-*b*-PCL concentrations of 0.5, 1.0, and 2.0 mg/ml were chosen for the assembly experiments because these concentrations were greater than the CMC values for PEG-*b*-PCL in water. The assembly of PEG-*b*-PCL (5000:4000) micelles was monitored using DLS (Fig. 2A). At all PEG-*b*-PCL (5000:4000) concentrations, no light scattering was detected at 100% ACN using DLS. Once the water content reached 10%, PEG-*b*-PCL (5000:4000) particles were detected using DLS at a PEG-*b*-PCL (5000:4000) concentration of 2.0 mg/ml and had an average hydrodynamic diameter of 140 nm. At 20% water content, the average hydrodynamic diameter of PEG-*b*-PCL (5000:4000) particles at this polymer concentration was increased to over 800 nm. At 30% water content, the hydrodynamic diameter of PEG-*b*-PCL (5000:4000) particles at 2.0 mg/ml decreased to 480 nm. It was after this point, at 40% water content, where the average hydrodynamic diameter of the PEG-*b*-PCL particles decreased to less than 50 nm. This dimension for PEG-*b*-PCL (5000:4000) particles was maintained even as the water content was increased further to 90%.

At lower polymer concentrations of 1.0 and 0.5 mg/ml, the hydrodynamic diameters of PEG-*b*-PCL (5000:4000) particles in ACN-water mixtures were similar to 2.0 mg/ml. However, the concentration of PEG-*b*-PCL (5000:4000) influenced the water content needed to induce assembly. The hydrodynamic diameter of PEG-*b*-PCL (5000:4000) at concentrations of 0.5 and 1.0 mg/ml was not detected until a 20% water content in ACN was reached. At this water content, the average hydrodynamic diameters of 0.5 and 1.0 mg/ml PEG-*b*-PCL particles were approximately 600 and 190 nm, respectively.

To examine the effect of the length of the core-forming block on ABC micelle assembly, the hydrodynamic diameters of PEG-*b*-PCL (5000:2500) and (5000:1000) particles in ACN-

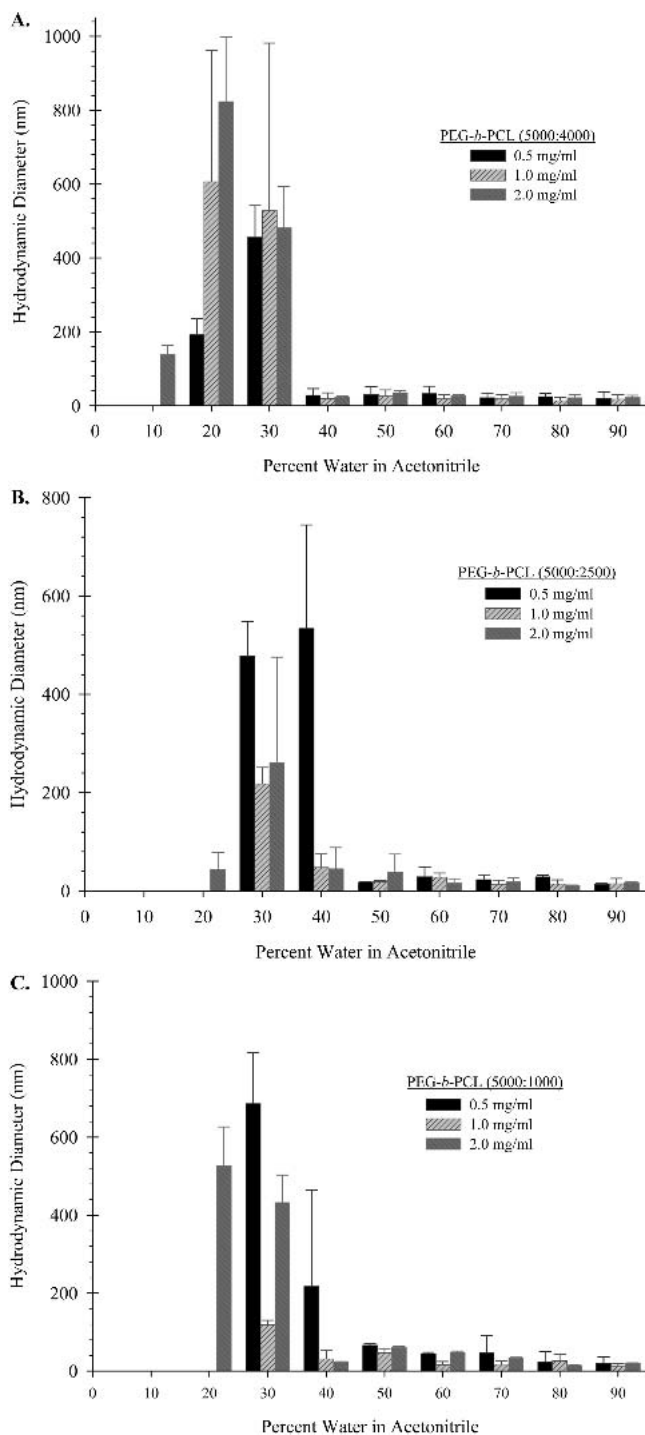


Fig. 2. The hydrodynamic diameters of PEG-*b*-PCL particles in ACN-water mixtures, which was monitored with DLS. The concentrations at each ACN-water composition were 0.5, 1.0, and 2.0 mg/ml. (A) PEG-*b*-PCL (5000:4000), (B) PEG-*b*-PCL (5000:2500), (C) PEG-*b*-PCL (5000:1000).

water mixtures were examined using DLS. Overall, the assembly of PEG-*b*-PCL (5000:2500) and (5000:1000) particles displayed the same trend as PEG-*b*-PCL (5000:4000) particles (Figs. 2B and 2C). The amount of water needed to induce PEG-*b*-PCL assembly again depended on PEG-*b*-PCL concentration. However, the assembly of PEG-*b*-PCL (5000:1000) and (5000:2500) unimers began at a higher water con-

centration than PEG-*b*-PCL (5000:4000) unimers. The hydrodynamic diameters of PEG-*b*-PCL (5000:1000) and (5000:2500) particles at concentrations of 2.0 mg/ml were first detected using DLS at 20% water content. At 30% water content, PEG-*b*-PCL (5000:1000) and (5000:2500) particles at concentrations of 1.0 and 0.5 mg/ml, were first detected using DLS. At 20–40% water content, PEG-*b*-PCL (5000:1000) and (5000:2500) particles reached large sizes of 200–800 nm before resulting in smaller and more monodispersed sizes near 50 nm at 50% water content. These distributions were maintained as water content was further increased.

When water was added to the solution of dissolved PEG-*b*-PCL in ACN, a significant increase in light scattering was detected using DLS, indicating the beginning of PEG-*b*-PCL assembly. The amount of water needed to induce ABC assembly has been termed the critical water content (CWC) (33). In ACN and water mixtures, the CWC of PEG-*b*-PCL particles was estimated at 10–30% water content, depending on PEG-*b*-PCL concentration and PCL block length. The dependence of the CWC value on the polymer concentration has been documented by Eisenberg with polystyrene-*b*-poly(acrylic acid) in *N,N*-dimethylformamide (DMF)-water mixtures (31). At higher polymer concentrations, ABCs will generally associate at lower water content.

At 10–40% water content, PEG-*b*-PCL unimers assembled into large structures with hydrodynamic diameters ranging from 200–800 nm. These dimensions were much larger than published diameters of PEG-*b*-PCL micelles in 100% water (22). This occurrence has also been reported with poly(*N*-isopropylacrylamide-co-dimethylacrylamide)-*block*-poly(D,L lactide) in dimethylacetamide (DMAc) and water mixtures, where the authors attributed this enhanced size to the swelling of hydrophobic cores with the organic solvent and water mixture (34). After enough water was added, the cores collapsed due to the decrease in solvent quality for the core-forming block, resulting in smaller dimensions that did not change appreciably as water content was increased.

To understand further the assembly of PEG-*b*-PCL particles in ACN and water, ¹H-NMR studies were performed. Through ¹H-NMR, resonances associated with the core and corona-forming blocks were monitored as a function of solvent composition. In ACN, the methylene protons of PEG block appear as a singlet at 3.6 ppm, as shown in Fig. 3. PCL block resonances appeared near 4.0, 2.1, 1.5, and 1.3 ppm and were labeled e, c, d, and d, respectively. ACN was found at 1.95 ppm. As water content increased, the PCL resonances broadened, whereas the peaks associated with PEG did not change; this occurrence has been attributed to ABC micelle formation (35). This suggests that the PCL portion of PEG-*b*-PCL associates with increasing water content and becomes the core of the PEG-*b*-PCL micelle. Using ¹H-NMR, it was determined that this event occurred at 30% water content, indicating that the CWC value for PEG-*b*-PCL (5000:4000) was near 30% water content. These data complement the DLS data, suggesting that the PCL block was important in PEG-*b*-PCL micelle assembly.

From the DLS and ¹H-NMR data, we can hypothesize the mechanism of PEG-*b*-PCL assembly. Our proposed model of PEG-*b*-PCL assembly in ACN-water mixtures is shown in Fig. 4. In 100% ACN, there was no detectable light scattering using DLS, and the ¹H-NMR peaks associated with PCL were not diminished or broadened, indicating that PEG-

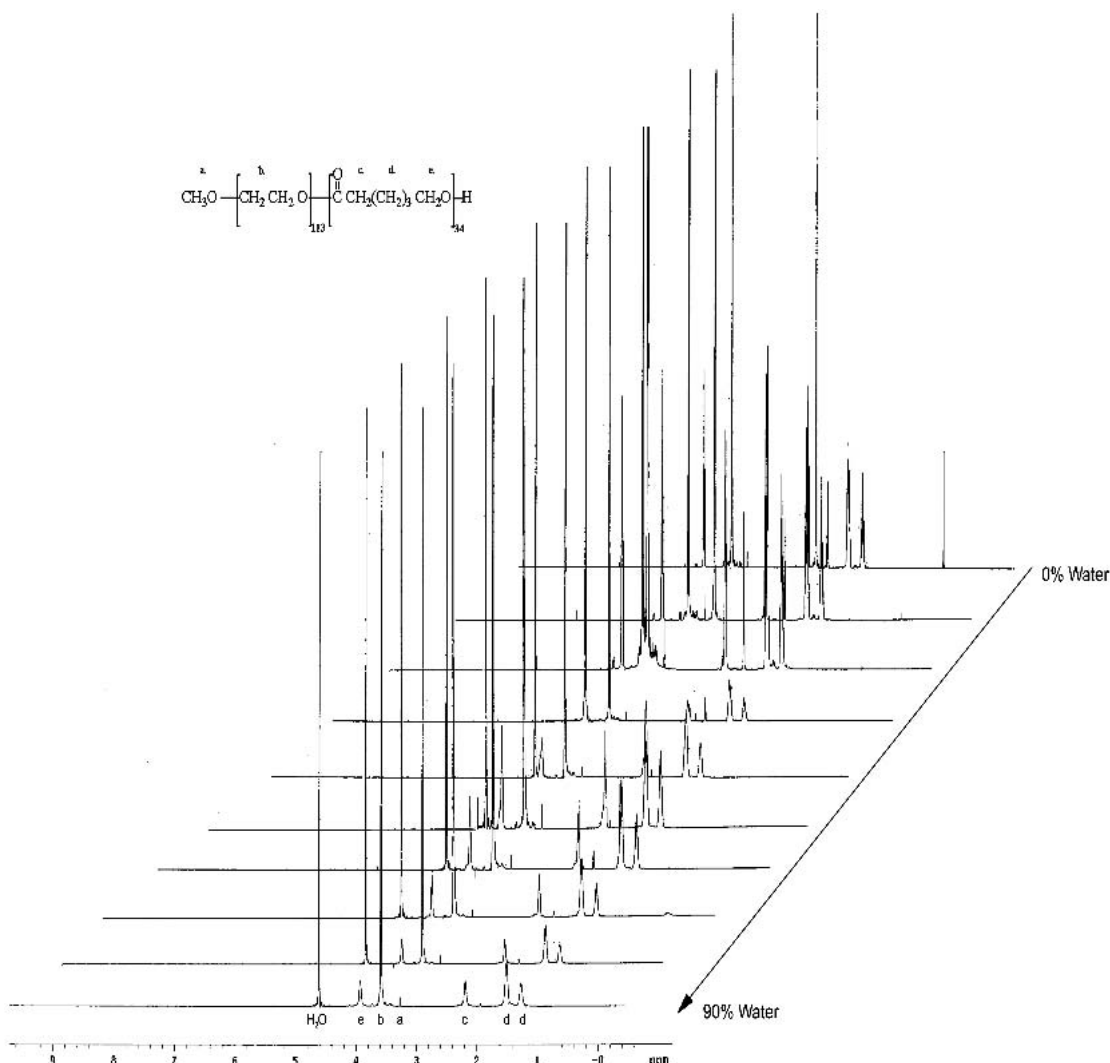


Fig. 3. $^1\text{H-NMR}$ spectra of PEG-*b*-PCL (5000:4000) in $\text{ACN-}d_3$ with gradual addition of D_2O , in 10% D_2O (v/v).

b-PCL exists as unimers. As water was added to the system, assembly of PEG-*b*-PCL unimers began between 10% and 40% water content, depending on PEG-*b*-PCL concentration and PCL block size. Through $^1\text{H-NMR}$, it was shown that the core of PEG-*b*-PCL particles was comprised of the PCL block. As water content was increased, PEG-*b*-PCL particles enlarged, possibly becoming swollen structures ranging from 200 to 800 nm in size. However, the possibility of other structures such as microemulsions or bicontinuous phases in this region cannot be discounted. With the further addition of

water, the PCL cores collapse and the sizes of these structures decreased. Beyond a water content of 50%, small PEG-*b*-PCL structures were observed. The particle size did not change as further water was added. At a water concentration higher than this, the ACN-water azeotrope was removed through evaporation, leaving behind an aqueous solution containing PEG-*b*-PCL micelles.

PEG-*b*-PCL Assembly with the Presence of Fenofibrate

Before preparing fenofibrate-loaded PEG-*b*-PCL micelles in water, it was necessary to determine what, if any, influence fenofibrate had on the PEG-*b*-PCL micelle assembly. This was important to determine the amount of water needed before removal of the ACN-water azeotrope. The assembly of PEG-*b*-PCL (5000:2500) and (5000:4000) micelles in the presence of 10% (w/w) fenofibrate was monitored using DLS, with experimental conditions identical to those in the absence of fenofibrate. DLS studies using PEG-*b*-PCL (5000:1000) were not performed because fenofibrate precipitate was observed at high water contents. This may indicate that PEG-*b*-PCL (5000:1000) micelles are not able to

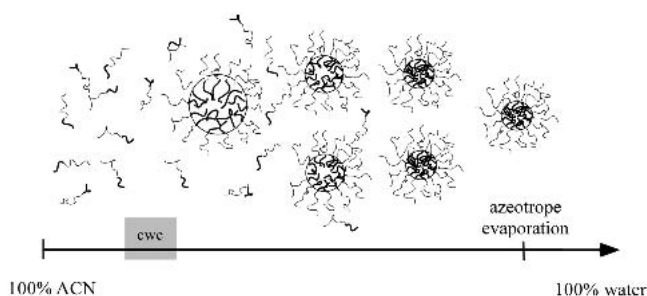


Fig. 4. Proposed model of PEG-*b*-PCL assembly.

encapsulate as much fenofibrate as PEG-*b*-PCL (5000:2500) and (5000:4000) micelles.

As shown in Fig. 5, the assembly profile of the ABCs, monitored with DLS, was similar to that without fenofibrate. PEG-*b*-PCL (5000:2500) and (5000:4000) structures at concentrations of 1.0 and 2.0 mg/ml were first detected using DLS at 10% water content. PEG-*b*-PCL (5000:2500) and (5000:4000) structures at 0.5 mg/ml were first detected at 20% water content. The large hydrodynamic diameters of the PEG-*b*-PCL particles occurred between 10% and 30% water content, with sizes between 200 and 1400 nm. At 40% water content, the sizes of PEG-*b*-PCL particles became smaller (under 50 nm) and more monodispersed.

It appeared that the assembly profile of PEG-*b*-PCL (5000:2500) and (5000:4000) micelles monitored with DLS was shifted toward lower water content compared to the previous assembly studies conducted in the absence of fenofibrate. At 10% (w/w) fenofibrate, the CWC was lowered. Upon further addition of water, the swollen structures decreased in size to under 50 nm and required less water for PEG-*b*-PCL (5000:2500) when fenofibrate was not present. Such results may be due to the hydrophobic interactions between fenofibrate and PCL. Therefore, fenofibrate assisted in the assembly of PEG-*b*-PCL.

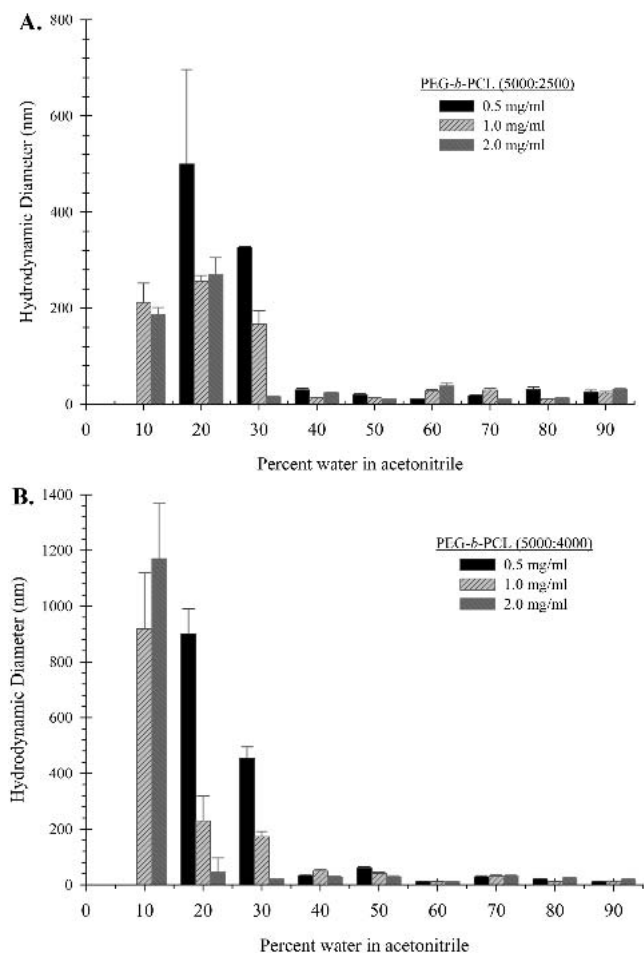


Fig. 5. Particle size of PEG-*b*-PCL with 10% w/w fenofibrate in ACN-water mixtures measured with DLS. (A) PEG-*b*-PCL (5000:2500); (B) PEG-*b*-PCL (5000:4000).

Fenofibrate Loading into PEG-*b*-PCL Micelles

Azeotropic removal through rotary evaporation was performed after the CWC. As shown in Table I, the average hydrodynamic diameters, measured with DLS, for all compositions of PEG-*b*-PCL micelles in water were below 50 nm. The sizes of the PEG-*b*-PCL micelles appeared to be dependent on the PCL block length. In 100% water, PEG-*b*-PCL (5000:4000) micelles had the largest size of approximately 35 nm. PEG-*b*-PCL (5000:2500) and (5000:1000) micelles were approximately 20 nm. In addition, the size distribution of PEG-*b*-PCL micelles after solvent removal also appeared dependent on PCL block size with PEG-*b*-PCL (5000:4000) micelles having the broadest size distribution. Fenofibrate loaded PEG-*b*-PCL micelles were all also less than 50 nm, shown in Table I.

The level of solubilized fenofibrate in order of increasing the PCL block size was 35, 100, and 90 $\mu\text{g/ml}$ respectively, which was much higher than the aqueous solubility of fenofibrate ($\sim 0.1 \mu\text{g/ml}$). In addition, PEG-*b*-PCL micelles prepared in this manner had higher fenofibrate levels than when prepared by dialysis because fenofibrate was not removed during the PEG-*b*-PCL micelle assembly process. The loading efficiency of fenofibrate into PEG-*b*-PCL micelles was determined by calculating the percentage of fenofibrate still associated with PEG-*b*-PCL micelles after filtration with 0.22- μm filter. Nearly a 90% loading efficiency was obtained with PEG-*b*-PCL (5000:4000) and (5000:2500) micelles, whereas PEG-*b*-PCL (5000:1000) micelles only obtained a loading efficiency of 29%. This was likely due to the smaller core of PEG-*b*-PCL (5000:1000) micelles compared to PEG-*b*-PCL (5000:4000) and (5000:2500) micelles.

SEC was used to verify the size of the PEG-*b*-PCL micelles, examine the stability and dissociation of the polymeric micelles upon dilution, and confirm fenofibrate loading. The SEC chromatogram of the PEG-*b*-PCL micelles, detected with refractive index, showed two peaks as shown in Fig. 6A. The first peak corresponds to 10^6 g/mol , which was consistent with ABC micelles; the second peak occurred in the 10^4 g/mol range, which corresponds to the molecular weight of the ABC unimers (8, 36). The determined M_w of the peaks differed depending on PCL content. PEG-*b*-PCL (5000:2500) and (5000:4000) micelles had larger peaks in the 10^6 g/mol range than in the 10^4 g/mol range. For PEG-*b*-PCL (5000:1000) micelles, the pattern was reversed, and the larger peak was in the unimer range of 10^4 g/mol . It appeared that an increased length of the PCL block led to greater the stability of the

Table I. Summary of PEG-*b*-PCL Micelle Size and Fenofibrate Loading Results

	PEG- <i>b</i> -PCL (5000:1000) micelles	PEG- <i>b</i> -PCL (5000:2500) micelles	PEG- <i>b</i> -PCL (5000:4000) micelles
No drug $2R_h$ (nm)	19 \pm 2	22 \pm 12	33 \pm 22
Loaded fenofibrate $2R_h$ (nm)	22 \pm 16	24 \pm 15	41 \pm 24
Fenofibrate loading efficiency (%)	29 \pm 9	95 \pm 2	92 \pm 3

Average hydrodynamic diameter of PEG-*b*-PCL micelles, with and without fenofibrate, as measured using DLS. The fenofibrate content associated with PEG-*b*-PCL micelles was measured using HPLC.

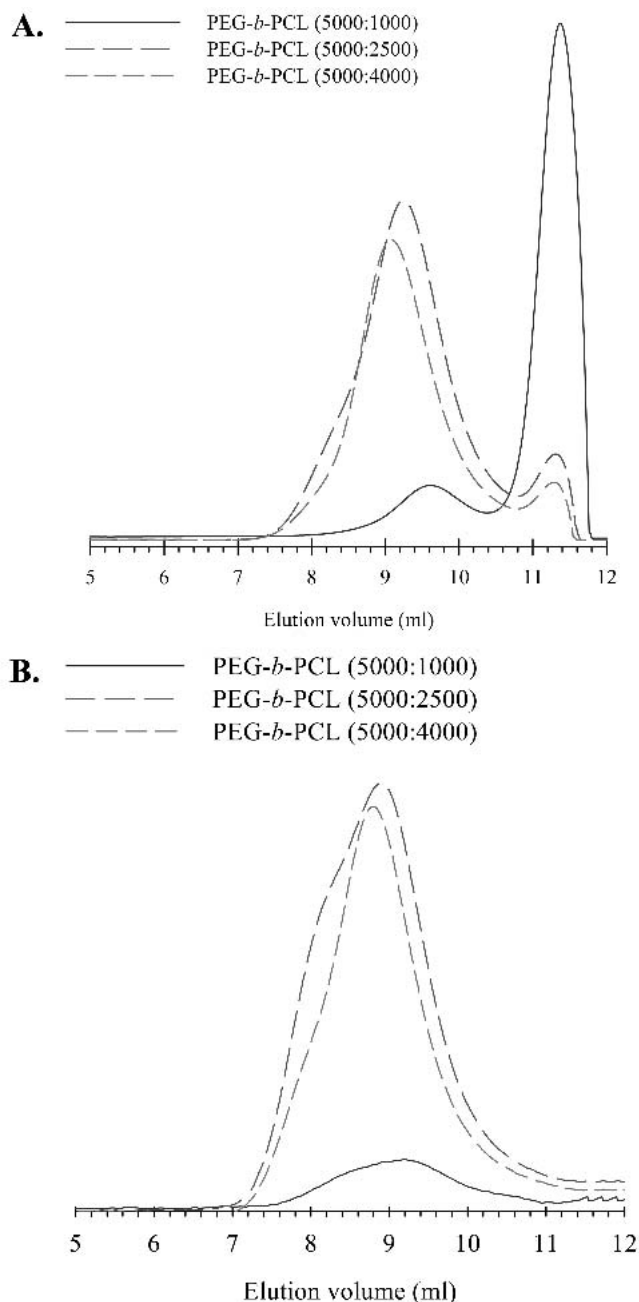


Fig. 6. SEC chromatogram of PEG-*b*-PCL (5000:1000), (5000:2500), and (5000:4000) micelles in water at 37°C with 10% (w/w) fenofibrate using (A) refractive index, (B) absorbance at 288 nm.

PEG-*b*-PCL micelle upon dilution. Fenofibrate, detected by monitoring the absorbance at 288 nm, eluted with PEG-*b*-PCL micelles, indicating encapsulation and retention of the drug upon dilution as shown in Fig. 6B.

CONCLUSIONS

Fenofibrate loaded PEG-*b*-PCL micelles were prepared by dissolving PEG-*b*-PCL and fenofibrate in ACN, followed by gradual addition of water, and subsequent removal of a negative ACN-water azeotrope with evaporation. The water content needed for PEG-*b*-PCL micelle assembly was influenced by PEG-*b*-PCL concentration, PCL block size, and the

presence of fenofibrate (10% (w/w)). With increasing water content, the average hydrodynamic diameter of PEG-*b*-PCL particles was increased, possibly due to the formation of swollen structures. As the water content increased further, the polydispersity and hydrodynamic diameters of PEG-*b*-PCL particles were lowered and PCL cores collapsed to form fairly monodisperse PEG-*b*-PCL micelles that did not change appreciably in size as water content was increased.

After azeotropic evaporation, aqueous PEG-*b*-PCL micelle solutions were obtained, and the sizes of PEG-*b*-PCL micelles increased slightly with the PCL block size. The PCL block size of PEG-*b*-PCL micelles was a factor in micelle stability when monitored with SEC. Using SEC, PEG-*b*-PCL (5000:2500) and (5000:4000) micelles eluted primarily in the 10^6 g/mol range, which was attributed to ABC micelles, rather than the 10^4 g/mol range, which was attributed to ABC unimers; whereas the situation was reversed for PEG-*b*-PCL (5000:1000) micelles.

It was possible using our assembly conditions to load fenofibrate into PEG-*b*-PCL micelles. Furthermore, the amount of fenofibrate encapsulated was dependent of the PCL block size. Micelle size and stability were similar in the presence or absence of fenofibrate at 10% (w/w).

ACKNOWLEDGMENTS

The authors would like to thank Ms. Monica Adams, School of Pharmacy, University of Wisconsin-Madison, for assistance with $^1\text{H-NMR}$. Abbott Laboratories generously provided financial support of this research. This work was also funded by the National Institutes of Health (AI-43346-02).

REFERENCES

1. K. Kataoka, G. S. Kwon, M. Yokoyama, T. Okano, and Y. Sakurai. Block copolymer micelles as vehicles for drug delivery. *J. Control. Rel.* **24**:119-132 (1993).
2. G. S. Kwon, M. Naito, K. Kataoka, M. Yokoyama, Y. Sakurai, and T. Okano. Block copolymer micelles as vehicles for hydrophobic drugs. *Colloids Surfaces B: Biointerfaces* **2**:429-434 (1994).
3. G. S. Kwon and K. Kataoka. Block copolymer micelles as long-circulating drug vehicles. *Adv. Drug Deliv. Rev.* **16**:295-309 (1995).
4. G. S. Kwon. Diblock copolymer nanoparticles for drug delivery. *CRC Crit. Rev. Ther. Drug Carrier Syst.* **15**:481-512 (1998).
5. G. S. Kwon and T. Okano. Soluble self-assembled block copolymers for drug delivery. *Pharm. Res.* **16**:597-600 (1999).
6. M.-C. Jones and J.-C. Leroux. Polymeric micelles- a new generation of colloidal drug carriers. *Eur. J. Pharm. Biopharm.* **48**:101-111 (1999).
7. C. Allen, D. Maysinger, and A. Eisenberg. Nano-engineering block copolymer aggregates for drug delivery. *Colloids and Surfaces B: Biointerfaces* **16**:3-27 (1999).
8. V. P. Torchilin. PEG-based micelles as carriers of contrast agents for different imaging modalities. *Adv. Drug Deliv. Rev.* **54**:235-252 (2002).
9. P. Wang, K. L. Tan, and E. T. Kang. Surface modification of poly(tetrafluoroethylene) films via grafting of poly(ethylene oxide) for reduction in protein adsorption. *J. Biomater. Sci. Polymer Ed.* **11**: 169-186 (2000).
10. R. Gref, M. Luck, P. Quellec, M. March, E. Dellacherie, S. Harnisch, T. Blunk, and R. H. Muller. 'Stealth' corona-core nanoparticles surface modified by the polyethylene glycol (PEG): influences of the corona (PEG chain length and surface density) and of the core composition on phagocytic uptake and plasma protein adsorption. *Colloids and Surfaces B: Biointerfaces* **18**: 301-313 (2000).

11. G. S. Kwon, S. Suwa, M. Yokoyama, T. Okano, Y. Sakurai, and K. Kataoka. Enhanced tumor accumulation and prolonged circulation times of micelle-forming poly(ethylene oxide-aspartate) block copolymer-adriamycin conjugates. *J. Controlled Release* **29**: 17–23 (1994).
12. M. L. Adams, A. Lavasanifar, and G. S. Kwon. Amphiphilic block copolymers for drug delivery. *J. Pharm. Sci.* **92**:1343–1355 (2003).
13. C. Allen, J. Han, Y. Yu, D. Maysinger, and A. Eisenberg. Polycaprolactone-*b*-poly(ethylene oxide) copolymer micelles as a delivery vehicle for dihydrotestosterone. *J. Controlled Release* **63**: 275–286 (2000).
14. X. Zhang, H. M. Burt, G. Mangold, D. Dexter, D. Von Hoff, L. Mayer, and W. L. Hunter. Anti-tumor efficacy and biodistribution of intravenous polymeric micellar paclitaxel. *Anticancer Drugs* **8**:696–701 (1997).
15. H. S. Yoo and T. G. Park. Biodegradable polymeric micelles composed of doxorubicin conjugated PLGA-PEG block copolymer. *J. Controlled Release* **70**:63–70 (2001).
16. A. V. Kabanov, E. V. Batrakova, and V. Y. Alakhov. Pluronic® block copolymers as novel polymer therapeutics for drug and gene delivery. *J. Controlled Release* **82**:189–212 (2002).
17. A. Lavasanifar, J. Samuel, S. Sattari, and G. S. Kwon. Block copolymer micelles for the encapsulation and delivery of amphotericin B. *Pharm. Res.* **19**:418–422 (2002).
18. A. Lavasanifar, J. Samuel, and G. S. Kwon. Micelles self assembled from poly(ethylene oxide)-*block*-poly(*N*-hexyl stearate L-aspartamide) by a solvent evaporation method: effect on the solubilization and haemolytic activity of amphotericin b. *J. Controlled Release* **77**:155–160 (2001).
19. K. Yu and A. Eisenberg. Multiple morphologies in aqueous solutions of aggregates of polystyrene-*block*-poly(ethylene oxide) diblock copolymers. *Macromolecules* **29**:6359–6361 (1996).
20. M. L. Adams and G. S. Kwon. The effects of acyl chain length on the micelle properties of poly(ethylene oxide)-*block*-poly(*N*-hexyl-L-aspartamide)-acyl conjugates. *J. Biomater. Sci. Polymer Ed.* **13**: 991–1006 (2002).
21. C. Allen, A. Eisenberg, J. Mrcic, and D. Maysinger. PCL-*b*-PEO micelles as a delivery vehicle for FK506: assessment of a functional recovery of crushed peripheral nerve. *Drug Delivery* **7**: (2000).
22. C. Allen, Y. Yu, D. Maysinger, and A. Eisenberg. Polycaprolactone-*b*-poly(ethylene oxide) block copolymer micelles as a novel drug delivery vehicle for neurotrophic agents FK506 and L-685,818. *Bioconjug. Chem.* **9**:564–572 (1998).
23. S. Y. Kim, Y. M. Lee, D. J. Baik, and J. S. Kang. Toxic characteristics of methoxy poly(ethylene glycol)/poly(ϵ -caprolactone) nanospheres; in vitro and in vivo studies in the normal mice. *Biomaterials* **24**:55–63 (2003).
24. S. Y. Kim, Y. M. Lee, H. J. Shin, and J. S. Kang. Indomethacin-loaded methoxy poly(ethylene glycol)/poly(ϵ -caprolactone) diblock copolymeric nanosphere: pharmacokinetic characteristics of indomethacin in the normal Sprague-Dawley rats. *Biomaterials* **22**:2049–2056 (2001).
25. S. Y. Kim, I. G. Shin, Y. M. Lee, C. S. Cho, and Y. K. Sung. Methoxy poly(ethylene glycol) and ϵ -caprolactone amphiphilic block copolymeric micelle containing indomethacin. II. Micelle formation and drug release behaviours. *J. Controlled Release* **51**: 13–22 (1998).
26. S. Y. Kim and Y. M. Lee. Taxol-loaded block copolymer nanospheres composed of methoxy poly(ethylene glycol) and poly(ϵ -caprolactone) as novel anticancer drug carriers. *Biomaterials* **22**: 1697–1704 (2001).
27. D. Law, W. Wang, E. A. Schmitt, Y. Qui, S. L. Krill, and J. J. Fort. Properties of rapidly dissolving eutectic mixtures of poly(ethylene glycol) and fenofibrate: the eutectic microstructure. *J. Pharm. Sci.* **92**:505–515 (2003).
28. J. A. Balfour, D. McTavish, and R. C. Heel. Fenofibrate: A review of its pharmacodynamic and pharmacokinetic properties and therapeutic use in dyslipaemia. *Drugs* **20**:260–290 (1990).
29. A. Lavasanifar, J. Samuel, and G. S. Kwon. The effect of alkyl core structure on micellar properties of poly(ethylene oxide)-*block*-poly(L-aspartamide) derivatives. *Colloids and Surfaces B: Biointerfaces* **22**:115–126 (2001).
30. G. S. Kwon, M. Naito, M. Yokoyama, T. Okano, Y. Sakurai, and K. Kataoka. Micelles based on AB block copolymers of poly(ethylene oxide) and poly(β -benzyl L-aspartate). *Langmuir* **9**:945–949 (1993).
31. L. Zhang, H. Shen, and A. Eisenberg. Phase separation behavior and crew-cut micelle formation of polystyrene-*b*-poly(acrylic acid) copolymers in solution. *Macromolecules* **30**:1001–1011 (1997).
32. L. H. Horsley. *Azeotropic Data-III*, American Chemical Society, Washington, DC, 1973.
33. Y. Yu, L. Zhang, and A. Eisenberg. Morphogenic effect of solvent on crew-cut aggregates of amphiphilic diblock copolymers. *Macromolecules* **31**:1144–1154 (1998).
34. F. Kohori, M. Yokoyama, K. Sakai, and T. Okano. Process design for efficient and controlled drug incorporation into polymeric micelle carrier systems. *J. Controlled Release* **78**:155–163 (2002).
35. Y. Li and G. S. Kwon. Micelle-like structures of poly(ethylene oxide)-*block*-poly(2-hydroxyethyl aspartamide)-methotrexate conjugates. *Colloids and Surfaces B: Biointerfaces* **16**:217–226 (1999).
36. M. L. Adams and G. S. Kwon. Relative aggregation state and hemolytic activity of amphotericin B encapsulated by poly(ethylene oxide)-*block*-poly(*N*-hexyl-L-aspartamide)-acyl conjugate micelles: effects of acyl chain length. *J. Controlled Release* **87**:23–32 (2003).